

Three-Phase Single-Stage Three-Level AC/DC Converter with A Wide Output Voltage Control Range

Eun-Soo Kim, Yechang Heo, Takongmo Marius, Jicheol Lee
Electrical and Electronics Engineering Jeonju University, Jeonju, Republic of Korea
Email: eskim@jj.ac.kr

Abstract— In this paper, a three-phase single-stage three-level AC/DC converter with a wide controllable output voltage is presented. The proposed converter integrates a PFC circuit and a three level DC/DC LLC circuit into one. Moreover, it operates at a fixed frequency and provides a wide controllable output voltage ($200V_{dc}$ - $430V_{dc}$) with a high efficiency over a wide load range. In addition, the input boost inductors operate in a discontinuous mode to improve the input power factor. The switching devices achieve ZVS, and the converter's THD is small. The feasibility of the proposed converter is verified with experimental results of a 2kW prototype.

I. INTRODUCTION

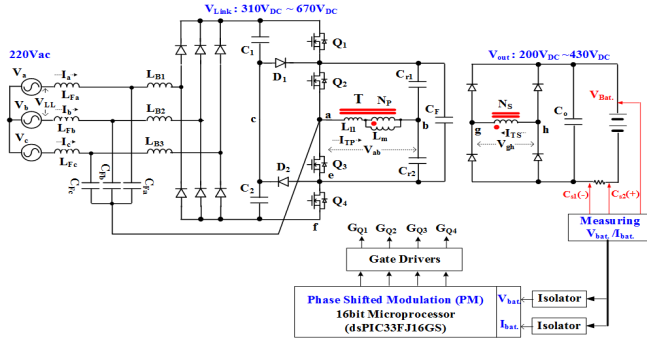
AC/DC converters are essential modules to connect DC loads to an AC grid. For high power and high voltage DC applications, three-phase AC/DC converters operating with ZVS and ZCS are required. Recent development of electric vehicle (EV) charging systems comprise of a front-end AC/DC topology such as three phase interleaved PFC converter, bridgeless PFC converter and three-phase VIENNEA rectifier, to improve the input power factor, followed by an isolated high frequency DC/DC three level resonant converter to regulate the output voltage[1]-[5]. However, such systems are two separate switch mode converters and thus the cost and size of the overall AC-DC converter is increased because of additional switching components with a complex control mechanism [6]- [7]. These drawbacks led to the emergence of single stage converters. However, previously published three-phase, three level phase shift (TL-PS) single stage AC-DC converters face problems of hard switching especially at low loads and it is difficult to have a controllable output voltage greater than twice the normal output voltage ($2V_o$) [8]. In addition, three level phase shift (TL-PS) single stage AC-DC converters have problems of high voltage stress on the secondary rectifier diodes, and low efficiency characteristics [9]-[10].

In this paper, we propose a three-phase three level single stage converter that mitigates these drawbacks. It improves the power density and efficiency of EV charging systems that operate within a wide range of controllable output voltage ($200V_{dc}$ - $430V_{dc}$).

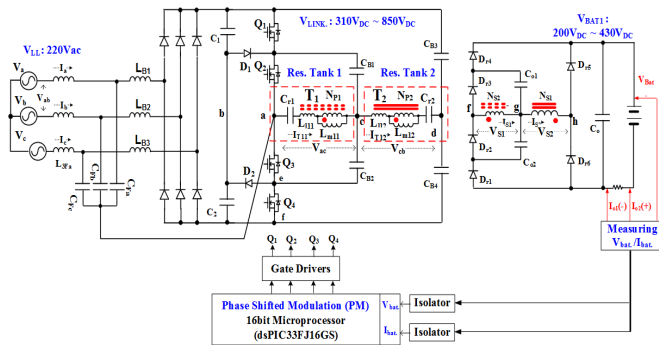
II. THE PROPOSED THREE-PHASE SINGLE-STAGE THREE LEVEL AC/DC CONVERTER

The proposed single stage converter is a three-phase three level AC/DC converter, which integrates an LLC resonant converter with a three-phase boost converter. Its theoretical analysis is verified with experimental results of a 2kW prototype whose output voltage ranges from $200V_{dc}$ to $430V_{dc}$. In addition, the system's total harmonic distortion rate (THD) is small and complies with standards [11]. Figure 1 shows the circuit diagrams of the proposed AC/DC three level converters. They are powered by a three phase AC source (V_{LL} : $220 V_{ac}$) and comprise of input filters (L_{Fa} - L_{Fc} , C_{Fa} - C_{Fc}), boost inductors (L_{B1} - L_{B3}), an input rectifier and a three level LLC resonant converter. The Filter capacitors (C_{Fa} - C_{Fc}) and filter inductors (L_{Fa} - L_{Fc}) are connected to the three-phase input to filter the input currents. The neutral point of the capacitors is connected between the source of switch Q_2 and the drain of switch Q_3 . The boost inductors (L_{B1} - L_{B3}) are connected to the input rectifiers and each pairs of the switching devices (Q_1 and Q_4) and (Q_2 and Q_3) in the primary side is alternately switched on and off with a fixed duty ratio of 50%. During the interval t_0 - t_1 (Q_1 & Q_2 are switched on) or t_4 - t_5 (Q_3 & Q_4 are switched on), the boost inductors (L_{B1} - L_{B3}) are energized according to the phase shift modulation of the three level converter. When the switching device Q_1 (or Q_4) is switched off during the interval t_2 - t_3 (or t_5 - t_6), the boost inductors (L_{B1} - L_{B2}) transfer their energy to the link capacitors C_1 and C_2 and their currents begin to reduce. The three level LLC resonant circuit of the first proposed converter shown in Figure 1(a) has only one transformer and 1/4 of the link voltage is applied across the terminals of the resonant circuit. When the outermost switches (Q_1 and Q_4) are switched off, all the boost inductor currents and resonant currents are forced to flow through (Q_2 and Q_3) and they suffer from high current stress, which affects the overall efficiency of the converter. To mitigate the drawback of high current stress on these switching devices (Q_2 and Q_3), a converter with two resonant circuits is proposed as shown in Figure 1(b). It consist of two transformers (T_1 , T_2) whose primary windings are connected in parallel while the

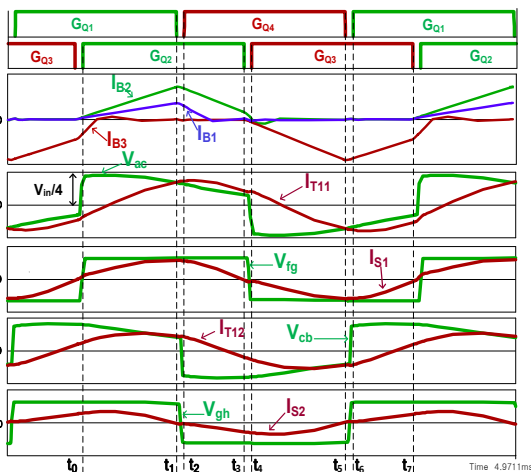
secondary windings are connected in series to ensure proper load sharing within the two transformers. The resonant circuits (Res. Tank 1, Res. Tank 2) equally operate at a constant switching frequency of Q_2 and Q_3 (Q_1 and Q_4), which alternately operate with a 50% duty and can vary the link voltage up to $850V_{dc}$. The boost inductor currents and resonant currents are shared between the two resonant circuits and mitigates the drawback of current stress in the first proposed circuit.



(a) Proposed 3-level AC / DC converter 1 and its control block diagram



(b) Proposed 3-level AC / DC converter 2 and its control block diagram



(c) Operating waveforms of the proposed 3-level AC/DC converter 2
Figure 1. The proposed single-stage 3-level AC/DC converter 2 and its operating waveforms

The increase in link voltage (V_{LINK}) reduces the current stress on the switching devices. $1/4$ of the link voltage (V_{LINK}) is applied across the primary windings of each transformers and a voltage according to the gain characteristic of the converter is applied to the secondary windings connected in series across the output diodes ($D_1 \sim D_6$). In addition, since the proposed three-phase single stage three-level AC/DC converters operate with a fixed frequency, the magnetizing inductances of the transformers (L_m) are designed to be considerably bigger than those in conventional resonant converters operating with variable frequency control mechanism. These high magnetic inductances limit the circulating currents and thus reduces conduction losses.

III. THE OPERATING MODES OF THE PROPOSED CONVERTER

Mode 1 ($t_0 \sim t_1$): In mode 1, the switching devices Q_1 and Q_2 are turn on. The filter capacitor voltages (V_{CFa} & V_{CFb}) are applied across the input boost inductors (L_{B1} & L_{B2}) and current flows from C_{Fa} & C_{Fb} through L_{B1} & L_{B2} , the input rectifier diodes, Q_1 & Q_2 and returns to C_{Fa} & C_{Fb} . The boost inductors (L_{B1} & L_{B2}), are energized while $1/4$ of the link voltage ($1/4V_{LINK}$) is applied across the primary terminals of the resonate circuits (Res. Tank 1, Res. Tank 2) and power is transfers to the secondary terminals. In addition, the boost inductor L_{B3} resets to zero.

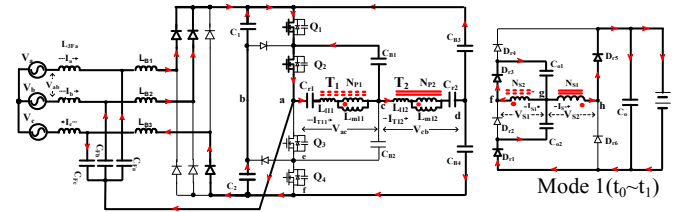


Figure 2: Current flow in mode 1 ($t_0 \sim t_1$)

Mode 2 ($t_1 \sim t_2$): At t_1 , Q_1 is switched off and its parasitic capacitor is charged while that of Q_4 is discharged. This mode ends when the voltage across the parasitic capacitor of Q_1 is clamped to half of the link voltage (V_{C1}) and when the voltage across the parasitic capacitor of Q_4 decreases to zero.

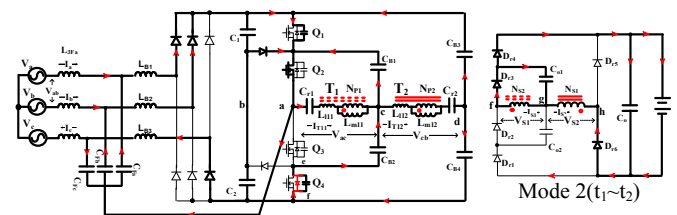


Figure 3: Current flow in mode 2 ($t_1 \sim t_2$)

Mode 3 ($t_2 \sim t_3$): This is a freewheeling stage; the switching device Q_1 is switched off and Q_4 is switched on with ZVS. In

addition, Q_2 remains on and the energy previously stored in the boost inductors is transferred to the link capacitors as current flows from C_{Fa} & C_{Fb} through L_{B1} & L_{B2} , the input rectifier diodes, link capacitor (C_1), clamping diode D_1 , Q_2 and back to C_{Fa} & C_{Fb} . During this period, the boost inductor currents begin to reset. Resonant current in Res. Tank 1 flows through Q_2 , C_{r1} , T_1 , C_{B1} and back to Q_2 , while resonant current in Res. Tank 2 flows through C_1 , C_{B3} , C_{r2} , T_2 , C_{B2} , and Q_4 .

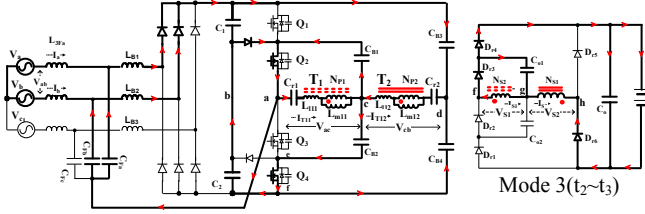


Figure 4: Current flow in mode 3 ($t_2 \sim t_3$)

Mode 4 ($t_3 \sim t_4$): In this mode, Q_2 is switched off and its parasitic capacitor begins to charge while that of Q_3 is discharged. This mode ends when the voltage across the parasitic capacitor of Q_2 is clamped to half of the link voltage and when the voltage across the parasitic capacitor of Q_3 decreases to zero.

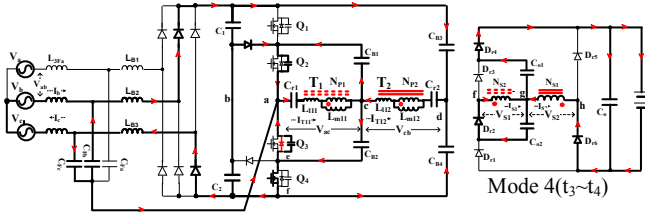


Figure 5: Current flow in mode 4 ($t_3 \sim t_4$)

Mode 5 ($t_4 \sim t_5$): In this mode, the switching devices Q_3 and Q_4 are on, the boost inductors (L_{B1} & L_{B2}) completely reset to zero while the boost inductor L_{B3} is energized as current flows from C_{Fc} through Q_3 & Q_4 , the input rectifier diode and L_{B3} . In addition, $1/4$ of the link voltage ($1/4V_{LINK}$) is applied across the primary terminals of the resonant circuits (Res. Tank 1, Res. Tank 2) and power is transferred to the secondary terminals.

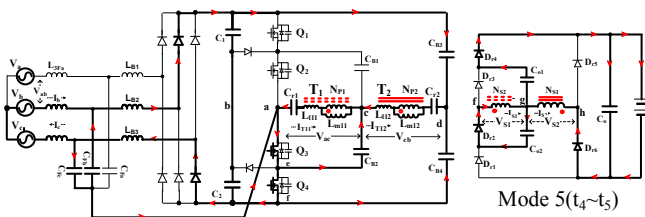


Figure 6: Current flow in mode 5 ($t_4 \sim t_5$)

Mode 6 ($t_5 \sim t_6$): At t_5 , Q_4 is switched off and its parasitic capacitor is charged to the voltage across C_2 . Simultaneously, the capacitor across Q_1 is discharged to zero. This mode ends

when the voltage across the parasitic capacitor of Q_4 is clamped to half of the link voltage (V_{C2}) and when the voltage across the parasitic capacitor of Q_1 decreases to zero.

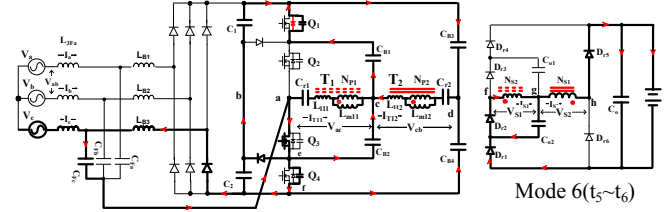


Figure 7: Current flow in mode 6 ($t_5 \sim t_6$)

Mode 7 ($t_6 \sim t_7$): This is a freewheeling stage; the switching device Q_4 is switched off and Q_1 is switched on with ZVS. In addition, Q_3 remains on and the energy previously stored in the boost inductors L_{B3} is transferred to the link capacitors as current flows from C_{Fa} through Q_3 , blocking diode, C_2 , the input rectifier diodes, L_{B3} , and back to C_{Fa} . During this period, the inductor current of L_{B3} begins to reset.

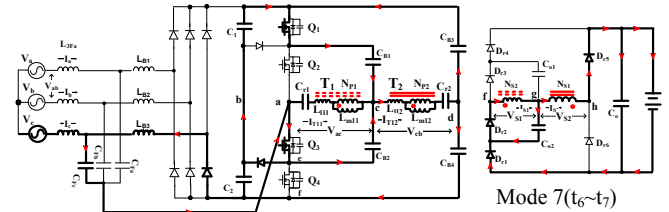


Figure 8: Current flow in mode 7 ($t_6 \sim t_7$)

IV. THE BOOST INDUCTOR AND TRANSFORMER DESIGN

A. BOOST INDUCTOR DESIGN

The boost inductors of single stage AC/DC converter required for high power applications are designed to operate in discontinuous mode (DCM). This is to ensure that the boost inductors ($L_{B1} \sim L_{B3}$) completely rest before the next switching cycle to shape the input current (I_a , I_b , I_c) so that they are sinusoidal. The power delivered to the output of the single stage converter is a function of the link voltage. In addition, the link voltage is a function of the boost inductance ($L_{B1} \sim L_{B3}$), switching frequency (f_s), peak input voltage (V_{pk}) and the phase shift (D). Equation (1) is a mathematical relationship of the voltage gain ($M_{(D,L)}$) of a three-phase single stage boost converter used to calculate the value of the boost inductor. Moreover, Figure 9 shows a three dimensional representation between the voltage gain ($M_{(D,L)}$), boost inductance ($L_{B1} \sim L_{B3}$) and the phase shift (D).

Let $L_{B1} = L_{B2} = L_{B3} = L_B$ and $T =$ the period

$$M_{(D,L)} = \frac{3 \left(3 + \sqrt{\frac{D^2}{(2L_B/T)^2}} \right)}{8} \quad (1)$$

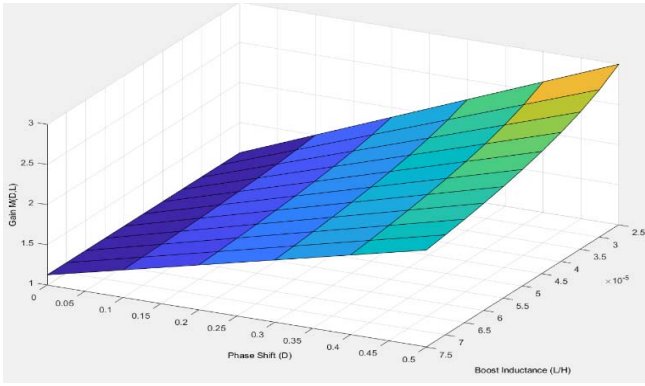


Figure 9: Voltage gain characteristics ($M_{(D,L)}$) due to the value of boost inductors and phase-shift(D) of a three-phase single stage AC/DC converter.

B. TRANSFORMER DESIGN

The proposed resonant converter operates at a constant frequency, thus the output voltage is directly proportional to the transformers turn ratio. The primary terminals of the resonant circuits (Res. Tank 1, Res. Tank 2) are connected in parallel while the secondary terminals are connected in series. Thus, the output voltage of the converter is the sum of the voltages across the secondary windings. The transformers are designed base on the conditions in which maximum current flows in the converter ($V_{LINK}=400V$ and $V_{out}=200V$). The equivalent circuit (Res. Tank 1) of one of the converter's resonant tanks is shown in Figure 10. Where L_{11} , L_{12} and L_m are respectively the primary leakage inductance, the secondary leakage inductance and the magnetizing inductance of transformer 1. Z_o is the output load and Z_p , Z_m and Z_s are respectively the primary, magnetizing and the secondary impedances of the resonant circuit. In addition, C_{r1} is the resonant capacitor, N is the turn ratio of transformer 1 and Z_i is the total impedance of one of the resonant circuits.

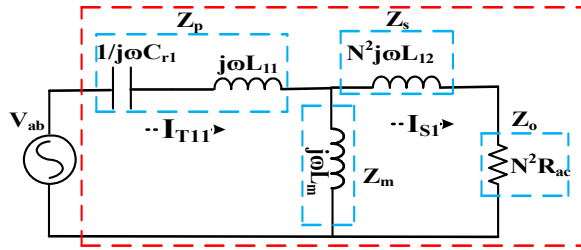


Figure 10: Equivalent circuit of LLC transformer

We assume that the two transformers are identical, that is

$$L_{L11} = L_{L12}, L_{m11} = L_{m12}, L_{s11} = L_{s12} \text{ and } L_{eq1} = L_{eq2}$$

The normalize voltage gain equation of the proposed converter is defined as follows;

$$G_v = \left[\frac{2}{1+A - \left(\frac{1}{\omega_n}\right)^2 \left(A + \frac{B}{1+B}\right) + jQ_m \left(\frac{1}{N^2} + \frac{B}{N^2}\right) + \left(\omega_n - \frac{1}{\omega_n}\right)} \right] \quad (2)$$

$$A = \frac{L_{11}}{L_m}, B = \frac{N^2 L_{12}}{L_m}, \omega_n = \frac{f_s}{f_r}, R_{ac} = \frac{8 * N^2}{\pi^2} R_L, Q_{Lm} = \frac{f_r L_{eq}}{L_m}$$

In addition, converter's gain characteristic curve for different controllable output voltage over a wide load condition is shown in Figure 11.

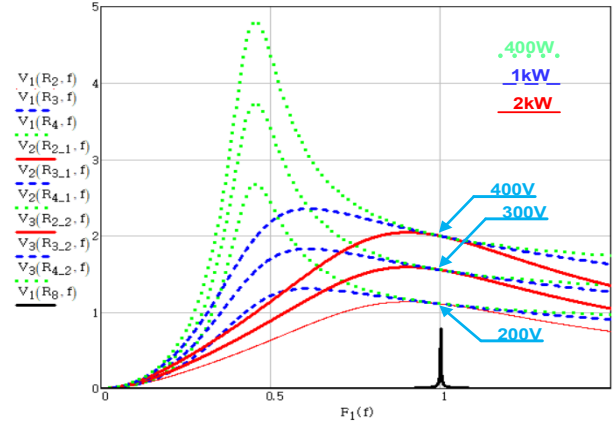


Figure 11: LLC converter gain characteristics

V. EXPERIMENTAL RESULTS

In order to verify the operation of the proposed converter, a 2kW three-phase single stage three level AC/DC converter with a wide output voltage range characteristic was designed and implemented.

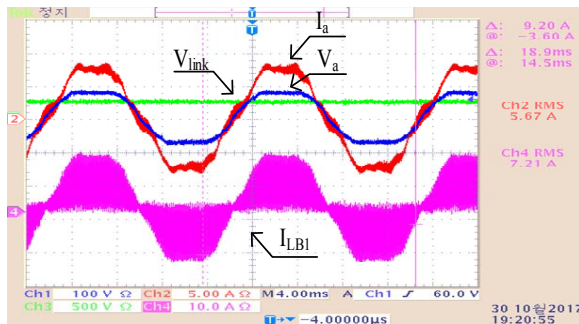
Table.1 Main ratings and transformer parameters

Main Rating	Input line voltage (V_{LL})	220V _{AC}	
	Output voltage(V_o)/ Output current(I_{omax})	200V _{DC} /10A, 430V _{DC} /4.65A (2kW)	
	Switching frequency(f_s)/ Resonance frequency(f_r)	108.29kHz/ 106.6kHz	
Used devices	Switching devices($Q_1 \sim Q_4$)	SCT3030AL (650V/70A/30m Ω)	
	Input rectifier diode	GP2D050A120B [1200V/50A/1.6V/SIC]	
	Input diodes($D_1 \sim D_2$)	GP2D050A060B [600V/50A/1.45V/SIC]	
	Output diodes	GP2D050A060B [600V/50A/1.45V/SIC]	
Parameters	$L_r \sim L_o / C_{Fr} \sim C_{Ff} / L_{B1} \sim L_{B3}$	0.94mH/2.86uF/35uH	
	$C_{r1} \sim C_{r2} / C_F$	200nF/2.2uF	
Transformer (T_1, T_2)	Primary/ Secondary inductance	L_p / L_s	55.6uH/56.1uH
	Equivalent leakage inductance	L_{eq}	56.1uH
	Turn ratio	$n_{b1} (N_{p1} / N_{s2})$	1(8T/8T)

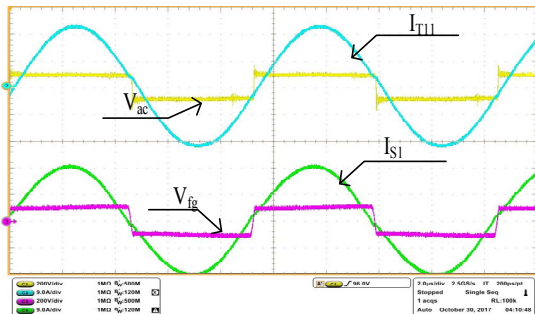
The proposed converter is controlled by a DSP algorithm using a 16-bit dsPIC33FJ16GS502 microcontroller that constantly senses the output voltage and current and operates the switching devices with a fixed frequency. The output voltage is controlled through phase shift. Table 1 shows the circuit's device ratings and transformers parameters.

Figure 12, Figure 13 and Figure 14 show the inductor currents (I_{LBI}), phase voltages (V_a), phase currents (I_a), link voltages (V_{LINK}) and primary voltages/ currents of the LLC resonant circuit (Res. Tank 1). Figure 15 shows the efficiency characteristics and total harmonic distortion (THD) curves of the proposed converter for different loads of each output voltage. Experimental results show that all the switching devices are switched on with ZVS especially at low loads. Moreover, the input currents have limited distortion.

Maximum efficiency characteristics were recorded with 500W load condition for all output voltage (200Vdc–430Vdc). A maximum efficiency of 94.4% was obtained with an output voltage of 200Vdc; moreover, an average efficiency of 91.58% was recorded. The lowest total harmonic distortion (THD) of 2.35% was obtained with a 2kW load when the converter operates with a 430Vdc output voltage.

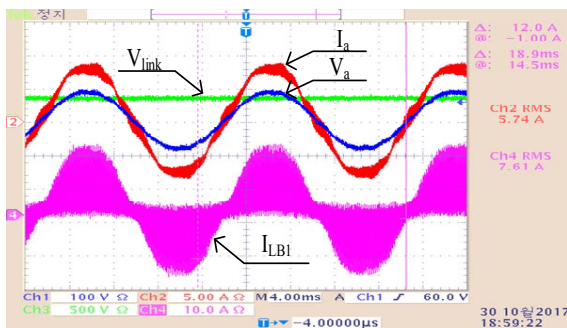


(a) Experimental waveforms of the PFC circuit.
Ch1:100V/div, Ch2:5A/div, Ch3:500V/div, Ch4:10A/div, 4ms/div

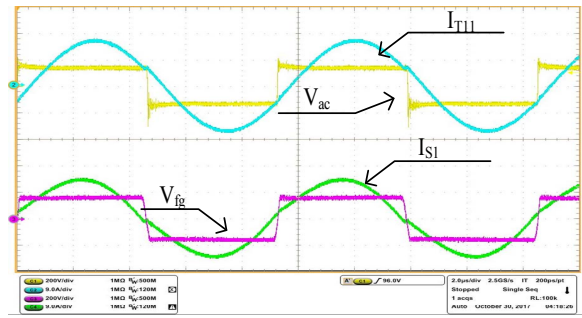


(b) The current and voltage waveforms across the transformer's primary and secondary windings
Ch1:200V/div, Ch2:9A/div, Ch3:200V/div, Ch4:9A/div, 2us/div.

Figure 12. Experimental waveforms for a 200V_{DC}/2kW converter.

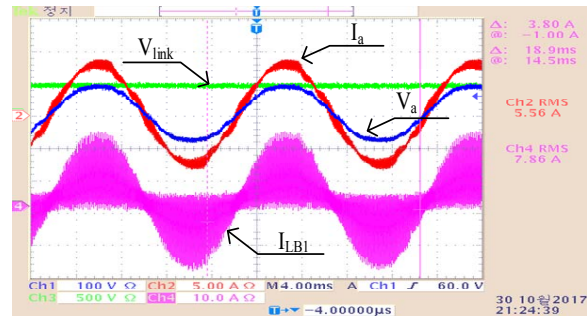


(a) Experimental waveforms of the PFC circuit.
Ch1:100V/div, Ch2:5A/div, Ch3:500V/div, Ch4:10A/div, 4ms/div

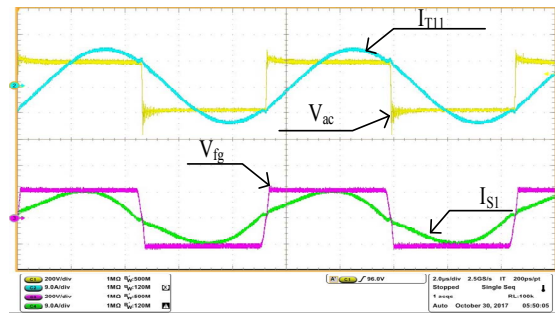


(b) The current and voltage waveforms across the transformer's primary and secondary windings
Ch1:200V/div, Ch2:9A/div, Ch3:200V/div, Ch4:9A/div, 2us/div.

Figure 13. Experimental waveforms for a 300V_{DC}/2kW converter



(a) Experimental wave forms of the PFC circuit.
Ch1:100V/div, Ch2:5A/div, Ch3:500V/div, Ch4:10A/div, 4ms/div



(b) The current and voltage waveforms across the transformer's primary and secondary windings
Ch1:200V/div, Ch2:9A/div, Ch3:200V/div, Ch4:9A/div, 2us/div.

Figure 14. Experimental waveforms for a 430V_{DC}/2kW converter

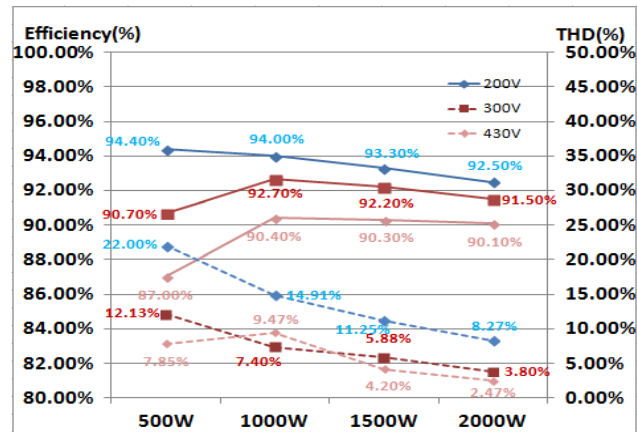


Fig. 15 Efficiency and THD characteristics in the proposed single stage three-level AC/DC converter

VI. CONCLUSION

A three-phase single stage three level converter with a wide controllable output voltage was presented. The proposed converter integrates a PFC circuit and a three level DC/DC LLC circuit into one. Moreover, it operates at a fixed frequency and provides a wide controllable output voltage ($200V_{dc}$ - $430V_{dc}$) with a high efficiency over a wide load range. In addition, all the switches are switched on with ZVS and the overall THD of the proposed converter is small.

REFERENCES

- [1] P. M. Barbosa, F. Canales, J. M. Burdio, F. C. Lee, "A Three Level Converter and Its Application to Power Factor Correction," IEEE Transactions on Power Electronics, Vol. 20, no.6, pp.1319-1327, November 2005.
- [2] Xinbo Ruan, "Fundamental Considerations of Three-Level Dc-Dc Converters: Topologies, Analyses, and Control," IEEE Transactions on Circuits and Systems—I: Regular Papers, Vol. 55, No. 11, pp.3733-3743, December 2008
- [3] S. Manias, R.Prasad, P.D. Ziogas, "A three-phase inductor fed SMR converter with high frequency insulation, high power density and improved power factor," in Proc. IEEE PESC, pp.253–263, 1987
- [4] R. Gules, A.S. Martins and I. Barbi, "A Switched Three-Phase Three-Level Telecommunications Rectifier," in INTELEC 1999, pp.29-3, 1999.
- [5] J. Contreras and I. Barbi, "A Three-Phase High Power Factor PWM ZVS Power Supply with a Single Power Stage," PESC'94, pp.356-362, 1994
- [6] G. Moschopoulos, "A simple AC–DC PWM full-bridge converter with integrated power-factor correction," IEEE Trans. Ind. Electron., vol. 50, no. 6, pp.1290–1297, Dec. 2003.
- [7] F. S. Hamdad and A. K. S. Bhat, "A novel soft-switching high-frequency transformer isolated three-phase AC-to- DC converter with low harmonic distortion," IEEE Trans. Power Electron., vol. 19, no. 1, pp.35–45, Jan. 2004.
- [8] Hiroyuki Haga, Fujio Kurokawa "Modulation Method of a Full-Bridge Three-Level LLC Resonant Converter for Battery Charger of Electric Vehicles"IEEE Transactions on Power Electronics, Vol. 32, no.4, pp.2498-2507, April 2017.
- [9] F. Alecks, M. Ford, M. Tuffs "Design of an Advanced High Power Density 1U Intelligent Rectifier of Electrical Vehicles" INTELECT.Twenty-second International Telecommunications Energy conference (cat. N0. 00CH37131), pp.17-23, 2000.
- [10] R. Gules, A.S. martins, I. Barbi "A Switched-Mode Three-Phase Three-Level Telecommunications Rectifier" Telle communication Energy conference, pp. 573, 1999.
- [11] Electromagnetic Compatibility—Part 3: Limits—Section 2: Limits forHarmonic Current Emissions (Equipment Input Current ≤ 16 A per Phase), IEC/EN 61000-3-2, 1995.